CASE STUDY

Novel approaches to Measure Receptor-Mediated Endocytosis of Herceptin

By Philip Auckland

3 OCTOBER 2023, 20 MIN READ

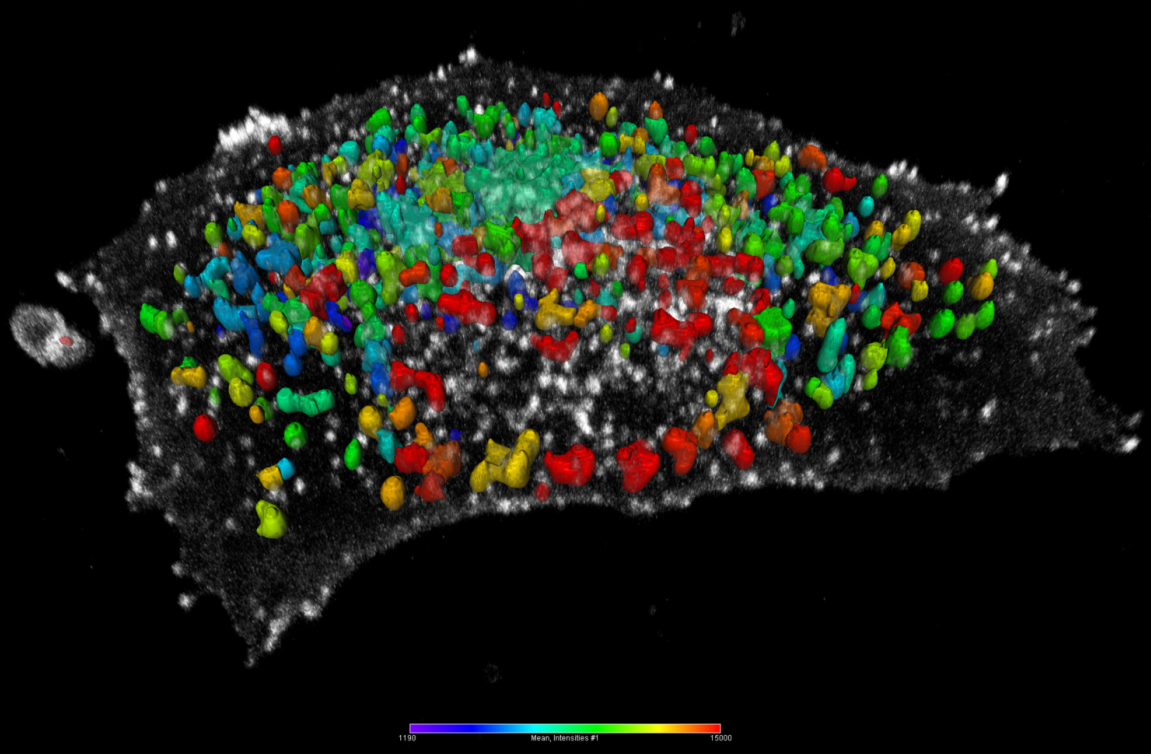

AUTHOR
Philip Auckland
Lead Scientist - Advanced Microscopy
Medicines Discovery Catapult

AUTHOR
Lorna Fitzpatrick
Lead Scientist in Cell and Molecular Engineering
Medicines Discovery Catapult

AUTHOR
Kang Zeng
Senior Scientist - Advanced Microscopy
Medicines Discovery Catapult

AUTHOR
Rebecca Kelly
Scientist - Advanced Microscopy
Medicines Discovery Catapult

AUTHOR
Aadarash Zia
Scientist - Drug Delivery
Medicines Discovery Catapult

AUTHOR
Philipp Seidel
Product Marketing Manager Life Sciences Software
ZEISS Microscopy

FROM IMAGE TO RESULTS

Novel Approaches to Measure Receptor-Mediated Endocytosis of Herceptin

In this series "From Image to Results", explore various case studies explaining how to reach results from your demanding samples and acquired images in an efficient way. For each case study, we highlight different samples, imaging systems, and research questions.

In this case study, we sought to develop a proof-of-concept assay that could quantify Herceptin plasma-membrane binding, internalization, and trafficking to late endosomes.

Case Study Overview

Sample	BT-474 cancer cell culture
Task	Implement novel receptor-mediated antibody internalization assay
Results	Completed assay proof-of-cocept for live imaging and 3D cell culture approaches
System	ZEISS LSM 880 with Airyscan
Software	ZEISS, ZEN, ZEISS arivis Pro

Introduction

In *vitro* characterization of complex medicines

In recent years, the focus of medical discovery has shifted from traditional small molecule approaches to complex therapies such as nanomedicines and biologics. Prior to application in vivo, the molecular dynamics and mechanism of these novel therapies must be thoroughly characterized in vitro. This not only helps to ensure efficacy and safety, but also advances the predictive capability of in vitro models and provides an avenue for the rational design of new medicines. In this study, Medicines Discovery Catapult (MDC), a non-profit medicines discovery organization in the United Kingdom, and ZEISS have developed an approach that combines genome engineering, advanced microscopy, and computational image analysis to quantify the plasma membrane binding, internalization and trafficking of Herceptin, an antibody-based complex medicine. We note that this approach is broadly applicable to other classes of complex medicines, such as silica nanoparticles, lipid nanoparticles, nucleic acids, and antibody-drug conjugates.

Antibody-based therapeutics have made valuable contributions to the treatment of cancer, autoimmune conditions, and aging-related disorders. Key to antibody-based approaches is the existence of a plasma membrane-bound or extracellular protein target whose function is critical to disease etiology.

Antibodies exert several effects when targeted to plasma membrane-bound receptors. In addition to directly blocking the receptor's natural ligand binding and preventing activation of the receptor's signaling cascade, receptor-bound antibodies can also provide an epitope for subsequent binding of immune cells and stimulate the Antibody-Dependent Cell-mediated Cytotoxicity (ADCC), whereby the target cell (e.g., a cancer cell) is destroyed. Antibody-bound receptors can also be internalized from the cell's surface by receptor-mediated endocytosis and then trafficked into the endolysosomal network. The latter process is key for a group of complex medicines called antibody-drug conjugates (ADC), which exploit the specificity of antibody-epitope binding to deliver a therapeutic payload intracellularly.

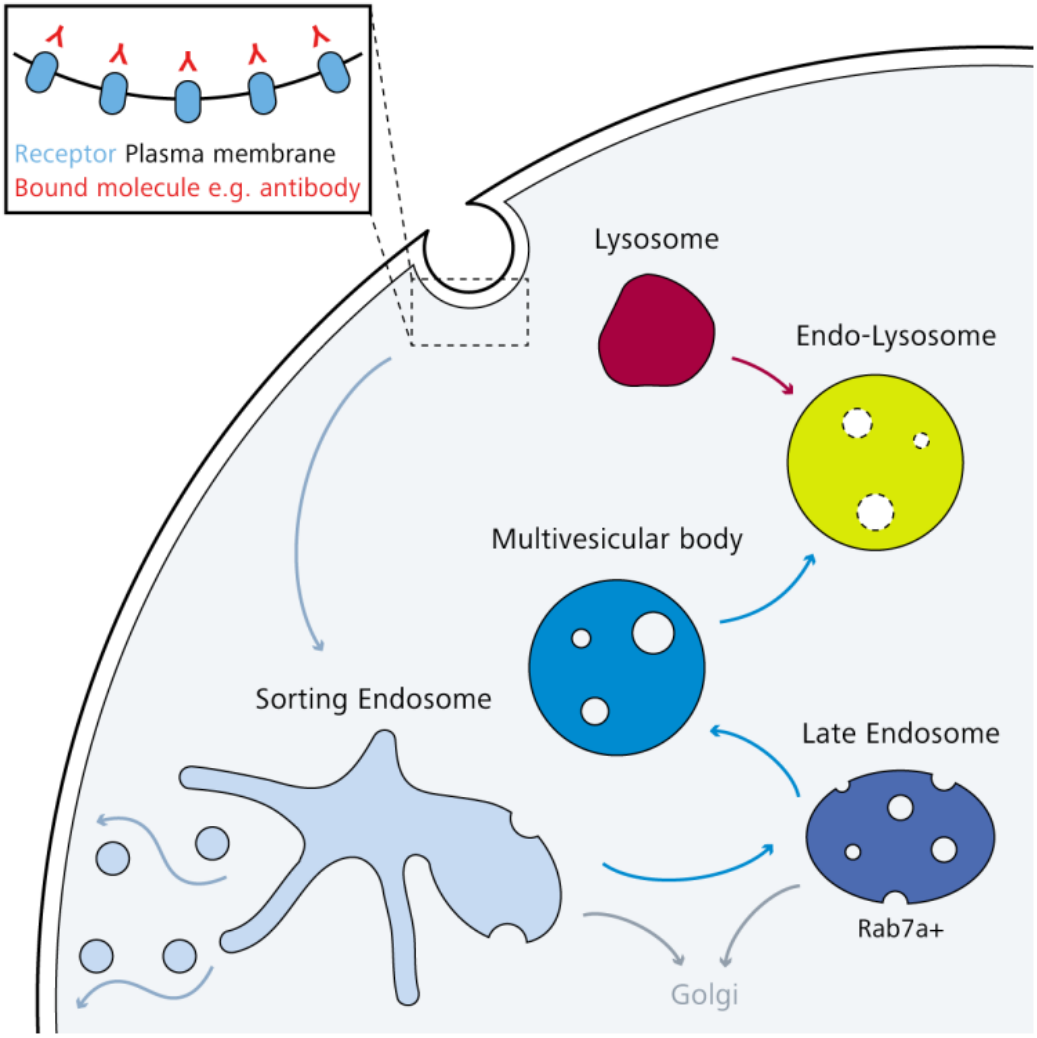

Figure 1: Schematic of antibody internalization and endolysosomal trafficking. The antibody (or other type of molecule) binds a plasma membrane-associated receptor. It is endocytosed into a membrane-bound vesicle and trafficked to a sorting endosome, where it can be recycled to the plasma membrane, transported to the Golgi, or retained as the compartment matures into a late endosome (note that these are Rab7a-positive). Late endosomes further mature into multivesicular bodies prior to fusion with a lysosome, which forms an endolysosome.

An assay for antibody binding, internalization, and trafficking

The efficacy of internalized antibody-based therapies is dependent upon a pathway that involves receptor binding, internalization, trafficking and, in some cases, release of a functional cargo (Figure 1). Understanding the molecular mechanism and kinetics of each step is key for therapeutic development, therefore, the field has developed assays to visualize internalization using fluorescence microscopy[1,2]. However, these assays lack spatiotemporal resolution and cannot distinguish between the myriad of trafficking pathways within the endolysosomal network. Further characterization of receptor-antibody internalization and trafficking thus requires the development of novel technologies.

We sought to develop a proof-of-concept assay that could quantify Herceptin plasma-membrane binding, internalization, and trafficking to late endosomes. Herceptin (also known as Trastuzumab) is an FDA-approved monoclonal antibody that binds human epidermal growth factor receptor 2, which is overexpressed in breast and stomach cancers. Herceptin meets many of the aforementioned mechanistic characteristics of therapeutic antibodies: it suppresses Her2 signaling by preventing receptor dimerization at the plasma membrane, triggers Her2 internalization and degradation and stimulates ADCC[3,4].

Cell Biology

BT-474 ductal carcinoma cells were used for all experiments. These cells are widely used in pre-clinical breast cancer research as a Her2-positive tumor model.

BT-474 GFP-Rab7a cell line was generated using TrueTag™ Donor DNA kit (Invitrogen™). Briefly, short homology arm primers (~50nt) were designed to target the N-terminus of Rab7a and used to prime the PCR amplification of the donor template. The template encoded a puromycin selection marker upstream of Emerald GFP separated by a P2A post-translational cleavage site. Cas9/single guide RNA and donor template were transfected into cells using Lipofectamine™ CRISPRMax™ as per the manufacturer's protocol.

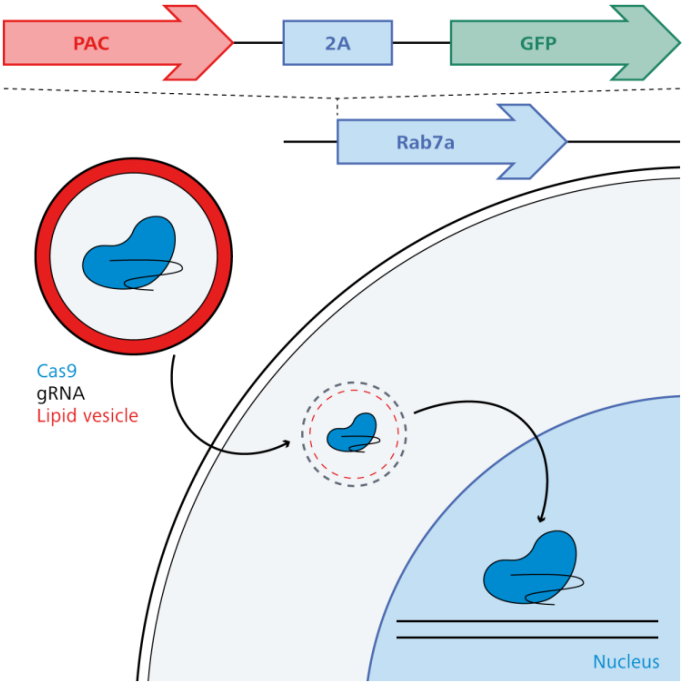

Figure 2: Cas9-mediated genome engineering to create eGFP-Rab7a cell line.

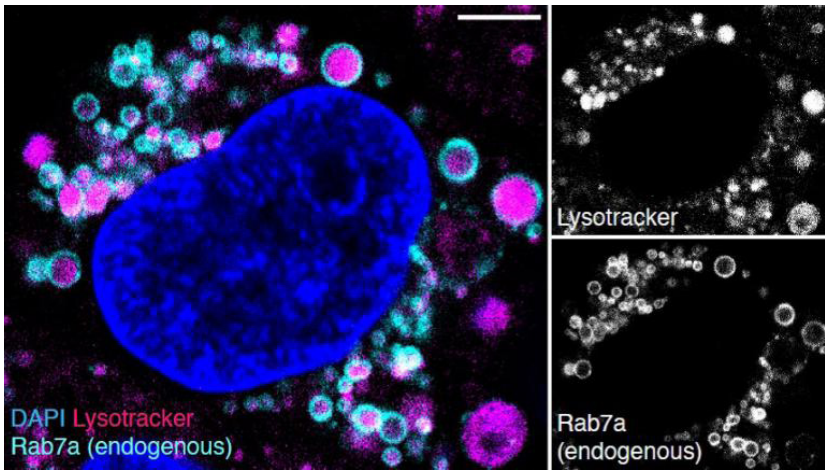

Figure 3: BT-474 cells were transfected with spCas9 protein complexed with a guide targeting exon 1 of Rab7a and a PCR donor cassette containing PAC-2A-GFP flanked by homology arms. eGFP-Rab7a positive cells were selected with puromycin. To confirm GFP knock-in and visualize correct eGFP-Rab7a localization, cells were fixed and stained with DAPI and Lysotracker.

48 hours post transfection, successfully knocked in cells were selected with puromycin at a concentration of 100 ng/ml. Knock-in at the target location was verified by Sanger sequencing and western blot. Figure 2 and 3 show the transfection scheme and images to validate co-localization of GFP-Rab7a-positive vesicles with lysosomal markers.

For spheroid formation, 10,000 BT-474 cells were grown overnight on a Costar U Cluster 96-well plate in DMEM containing 10% FCS

Image Acquisition

For sample preparation, BT-474 GFP-Rab7a cells were seeded on 8-well chamber slides (ibidi 80826) and grown for at least 24 hours.

For RNAi, 10 pmol of Her2 or control siRNA (Thermo Fisher) was added to 50 µl OptiMEM containing 0.3 µl Lipofectamine RNAiMAX (Invitrogen), incubated at room temperature for 20 minutes then added to cells for 48 hours.

For priming with Trastuzumab-AF647 (TZ-AF647; Novus Biologicals), cells were washed with cold serum-free DMEM and incubated with 10 µg/ml TZ-AF647 in serum-free DMEM at room temperature for 15 minutes. As controls, 10 µg/ml Transferrin-AF647 (Jackson ImmunoResearch) or 20 µg/ml of AF647-labelled goat anti-human secondary antibody (Invitrogen A-21445) was used in place of TZ-AF647. Clathrin-mediated endocytosis was inhibited with 30 µM Pitstop 2 (Abcam ab120687) for 30 minutes prior to addition of TZ-AF647. After antibody incubation, cells were washed once and cultured with warm complete DMEM.

Imaging was performed using Airyscan in confocal mode (increased sensitivity to detect weak signals) on the ZEISS LSM 880 confocal microscope equipped with a Plan-Apochromat 20x 0.8 NA objective, humidified chamber and incubator that maintained 37°C and 5% CO2. For live imaging, Definite Focus 2 was used to avoid focus drift. A single plane was acquired every 7 minutes for 4 hours. For spheroid imaging, Z-stacks were acquired on the LSM 880 confocal system described above with optimized Nyquist sectioning (0.5 µm for high-resolution image data).

Software Processing

For image analysis, the task was finding an optimal read-out for internalization and trafficking of Trastuzumab to GFP-Rab7a late endosomes. To this end, we segmented both Trastuzumab (TZ-AF647) puncta and GFP-Rab7a-positive endosomes to compare different approaches.

Analysis for TZ-AF647 was straight-forward. We applied Blob Finder segmentation (vesicle diameter ~ 1 µm) and filtered out very small segments (< 0.4 µm²). This operation successfully identified both internalized and plasma membrane-bound TZ-AF647.

To identify late endosomes using GFP-Rab7a, we first normalized and denoised the data to avoid variation in GFP intensity affecting correct segmentation of endosomal vesicles. Next, we employed the Blob Finder segmentation (vesicle diameter ~ 1.5 – 2 µm) to generate raw GFP-Rab7a-positive segments. To ensure that all endosomal vesicles were entirely segmented (Rab7 only localizes to endosomal membranes), we used morphological closing and hole filling. Finally, very small segments (< 0.4 µm²) were filtered out.

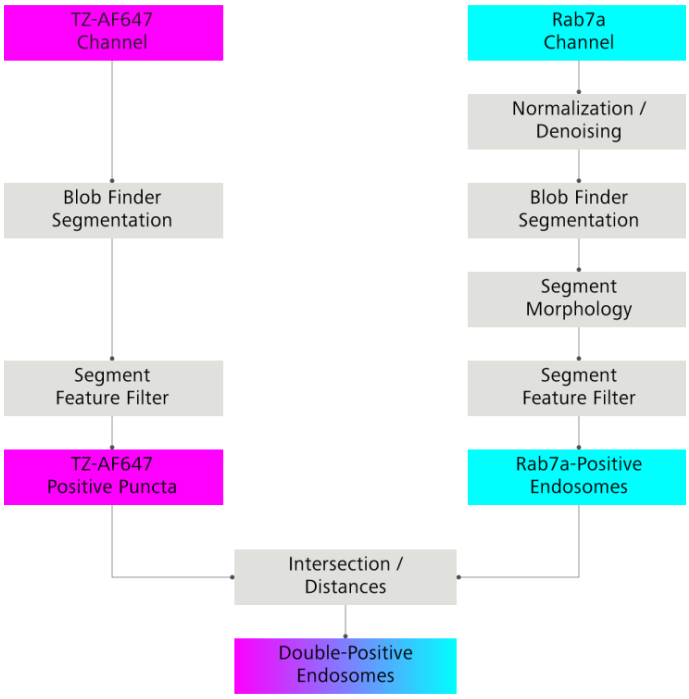

Image Analysis Pipeline in ZEISS arivis Pro

Having segmented both TZ-AF647 puncta and GFP-Rab7a vesicles, we used the Object Distance and the Object Intersection functions to measure the spatial overlap of both object groups. In this analysis, we have looked at several data sets, including data from fixed cells, time-lapse imaging and 3D spheroids. All were analyzed with this principal strategy, but analyses differed in their details as outlined in the results section.

Validation

A key concern for the image processing steps of the experiment was if TZ-AF647 puncta and GFP-Rab7a-positive endosomes were segmented to sufficient quality and specificity for quantification. Figure 4 and 5 show comparisons of raw images and resulting segments for TZ-AF647 and GFP-Rab7a, respectively. Both membrane-bound and internalized TZ-AF647 were reliably detected.

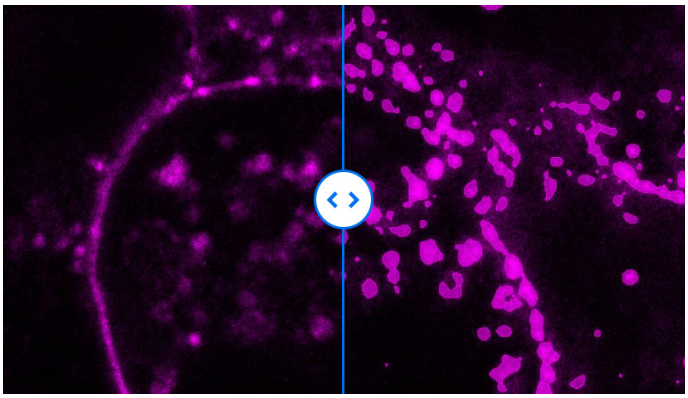

Figure 4: Segmentation quality for TZ-AF647. Raw TZ-AF647 shown on the left, TZ-AF647 segments shown on the right of the slider. Both membrane-bound and internalized TZ-AF647 were reliably detected.

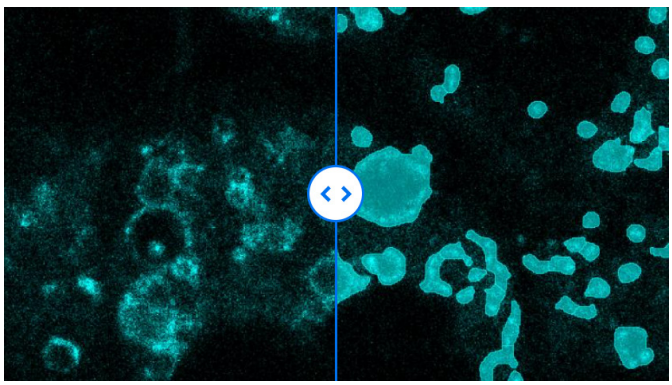

Figure 5: Segmentation quality for GFP-Rab7a. Raw GFP-Rab7a is shown on the left slider and Rab7a segmentation is shown on the right slider. Most, but not all the identified endosomes, were detected in their entirety.

For GFP-Rab7a the segmentation was more difficult, because it localizes to the endosomal membrane and the endogenous labelling strategy yields a lower signal-to-noise ratio. Nevertheless, by using morphological operations (dilation and hole filling), late endosomes were clearly identifiable using the endogenous GFP-Rab7a signal.

Results

Quantifying Trastuzumab-AF647 Association with Late Endosomes

To establish an optimal read-out for TZ-AF647 association with late endosomes, we treated endogenous eGFP-Rab7a expressing BT-474 cells with TZ-AF647 or Transferrin-AF647 for 30min prior to fixation. To confirm that TZ-AF647 and Transferrin-AF647 were internalized by endocytosis, we incubated cells with Pitstop 2, an inhibitor of clathrin-mediated endocytosis (Figure 6). We then sought to develop an automated image analysis pipeline to distinguish plasma membrane-bound from intracellular TZ-AF647 and then quantify the colocalization of TZ-AF647 and GFP-Rab7a.

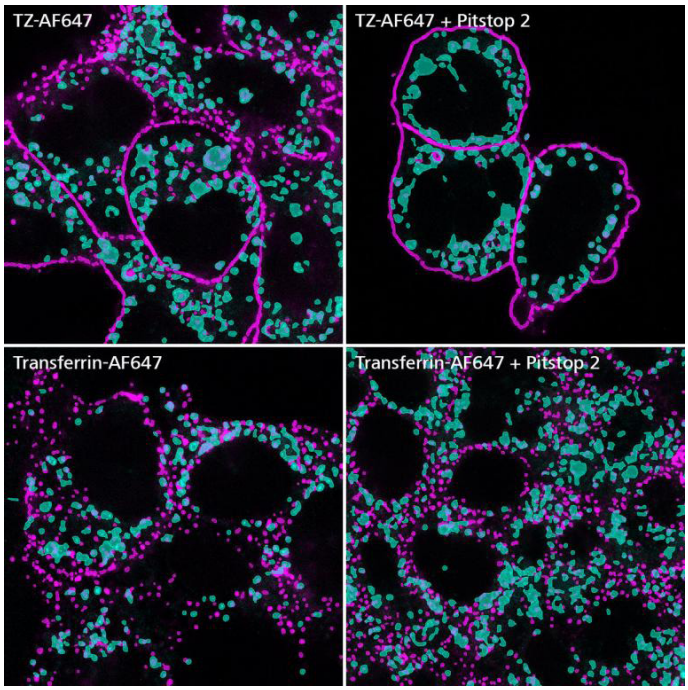

Figure 6: BT-474 eGFP-Rab7a cells treated with TZ-AF647 or Transferrin-AF647 and Pitstop 2. BT-474 cells expressing endogenously-labeled eGFP-Rab7a were treated with DMSO or 30 µM Pitstop 2 for 30 minutes before incubation with 10 µg/ml TZ-AF647 or Transferrin-AF647 for 15 minutes.

We tested two strategies for quantification of TZ-AF647 colocalization with late endosomes.

First was a "proximity-based" approach that used the Distance function of ZEISS arivis Pro to determine the minimal distance between individual TZ-AF647 puncta and GFP-Rab7a-positive endosomes. This approach led to the unexpected result that internalized TZ-AF647 increased in Pitstop 2 treated cells, which is likely an analysis artifact due to the proximity of some Rab7a vesicles to the plasma membrane.

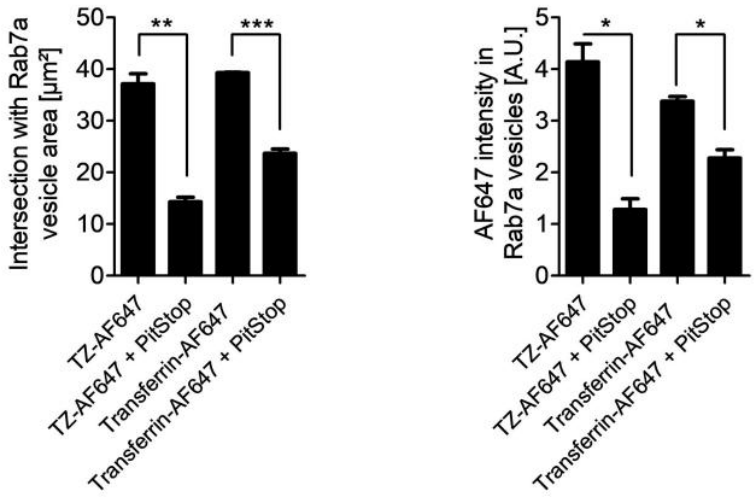

Figure 7: Segment-based read-outs for TZ-AF647 endocytosis. The left plot shows the area of overlapping TZ-AF647 puncta and GFP-Rab7a vesicles. The right plot shows the total AF647 intensity in GFP-Rab7a vesicles. Error bars indicate the s.e.m. of two independently analyzed fields of view. Student's t-test between pairs of samples with and without PitStop. * p = 0.05; ** p = 0.01; *** p = 0.001.

The other was a "segment-based" approach (Figure 7). Here, we determined: (i) the object intersection between intracellular TZ-AF647 puncta and GFP-Rab7a-positive endosomes, or (ii) the TZ-AF647 intensity within GFP-Rab7a-positive endosomes. The latter approach was the most decisive in terms of depicting the differences between untreated and Pitstop 2-incubated samples.

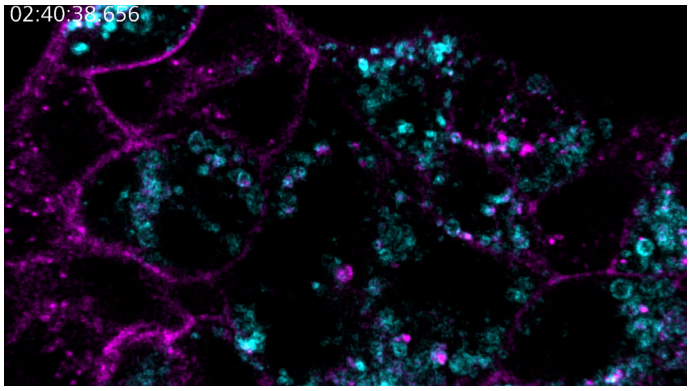

Quantifying Trastuzumab-AF647 Trafficking to Late Endosomes in Live Cells

Next, we aimed to visualize TZ-AF647 trafficking to late endosomes via live imaging. To this end, we imaged GFP-Rab7a expressing cells treated with control siRNA and 10 µg/ml TZ-AF647 every 7 minutes for 4 hours.

This revealed that intracellular TZ-AF647 puncta formed over time and began to co-localize with GFP-Rab7a, suggesting that TZ-AF647 was being endocytosed and trafficked through the endosomal network (video above). Consistent with this, cells treated with RNAi against the Trastuzumab receptor Her2 (that depleted the protein by 74%), showed reduced plasma-membrane-bound and intracellular TZ-AF647 (video to the right/below).

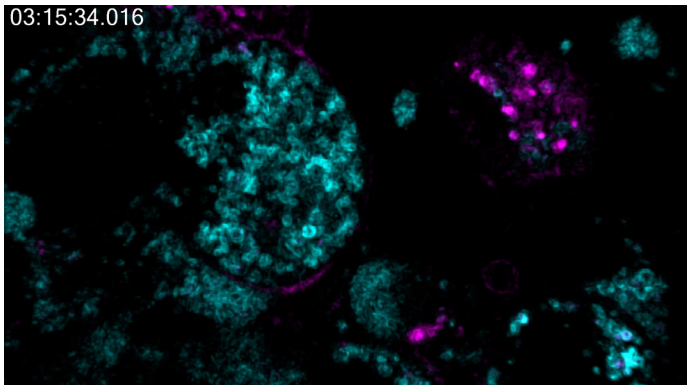

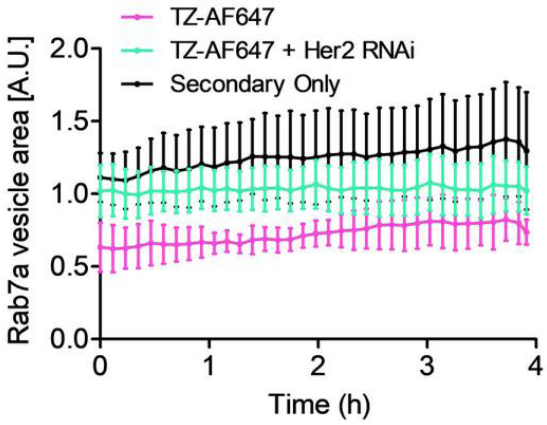

Figure 8: Relative areas of segmented GFP-Rab7a endosomes over time. Note that the total area of GFP-Rab7a segments is stable within samples but varies between samples. Error bars indicate s.e.m. of n=2 biological repeats.

To quantify TZ-AF647 trafficking to GFP-Rab7a-positive endosomes as precise as possible, we accounted for two experimental variables. First, as the amount of initial plasma-membrane-bound TZ-AF647 is subject to variation, all quantification has been corrected for the t=0min minimal fluorescence intensity values. Second, since the total amount of detected vesicles might differ between samples (Figure 8), we normalized intensity measurements for total vesicle area.

Figure 9 shows the pooled data from four biological repeats of our live imaging experiments of TZ-AF647 internalization. These revealed that TZ-AF647 begins to co-localize linearly with GFP-Rab7a late endosomes ~30 minutes after addition, reaching the maximal observed value four hours post incubation (when imaging stopped). In cells treated with Her2 siRNA, TZ-AF647 colocalization with GFP-Rab7a endosomes was also observed at ~30 minutes, however its accumulation was severely attenuated (~70% reduction at t=4 h, Fig 10). Together, these data establish that the endocytosis and intracellular trafficking of TZ-AF647 to late endosomes can be reliably followed by live-cell imaging.

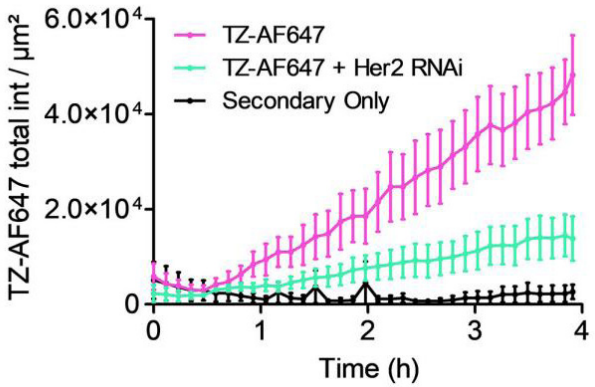

Figure 9: TZ-AF647 accumulation in GFP-Rab7a endosomes over time. Raw TZ-AF647 intensities were normalized for t=0 min background intensity and total GFP-Rab7a area per sample. Error bars indicate s.e.m. of n=4 biological repeats.

Quantifying TZ-AF647 Internalization in Cancer Spheroids

3D cancer spheroids represent an experimental model that is more physiologically relevant than 2D cell culture with the benefit of being cheaper and more scalable when compared to in vivo experimentation.

To understand whether our approach could quantify TZ-AF647 internalization in cancer spheroids, we grew BT-474 cells into spheroids with an approx. diameter of 400 µm and incubated them with 10 µg/ml TZ-AF647 for 24 h. In line with our 2D cell culture experiments above, we found that TZ-AF647 localized to the plasma membrane at t=0 h and formed intracellular puncta by t=24 h (Figure 10). We note that with the current confocal setup as described in the methods section, useful resolution can only be obtained at the surface of the spheroid (depth ~ 30 µm).

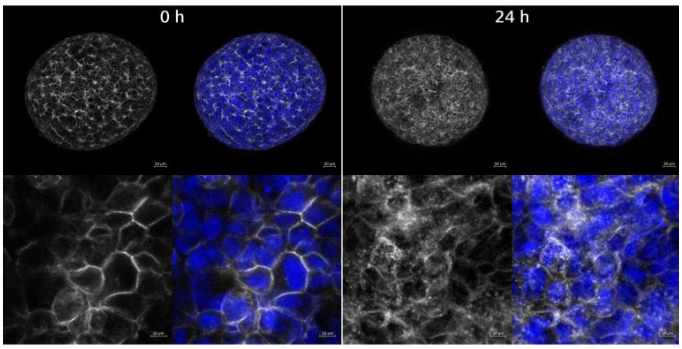

Figure 10: TZ-AF647 internalization in BT-474 cancer spheroids. BT-474 spheroids were fixed immediately and 24 hours after TZ-AF647 exposure and imaged in 3D (Maximum Intensity Projection shown here). Overview images shown in upper row (scaling of 1.38 µm / pixel) and detailed images shown in lower row (scaling of 0.21 µm / pixel). Notice the striking shift between TZ-AF647 membrane association at t = 0 hours and intracellular localization at t = 24 hours.

For quantification, cells in spheroids were detectable at sufficient resolution to perform TZ-AF647 segmentation with Blob Finder as above. However, in the absence of an endosomal marker, we used a different strategy to roughly distinguish membrane-bound from internalized TZ-AF647 based on segment volume with a cutoff value of 5000 voxels (Figure 11).

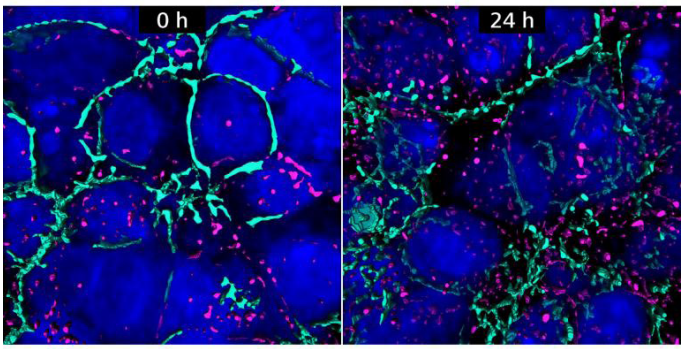

Figure 11: Distribution of TZ-AF647 on cancer spheroids based on image analysis. TZ-AF647 was first segmented with Blob Finder (with deactivated splitting). Segments were then subclassified into endosome- and membrane-associated TZ-AF647 based on segment volume (membranes with more and endosomes with less than 5000 voxels). Maximum intensity rendering of 3D volume is shown.

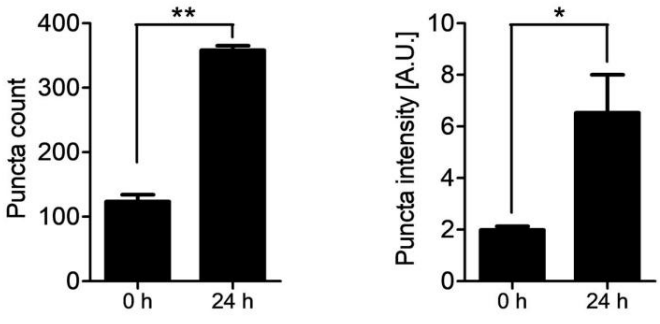

Figure 12: TZ-AF647 internalization over time. Quantitative read-out of segments from figure XXY. Both internalized puncta count and AF647 sum intensity are markedly higher 24 hours post TZ-AF647 exposure. Error bars indicate the s.e.m. of two independently analyzed fields of view. Student's t-test between pairs of sample with and without PitStop. * p = 0.05; ** p = 0.01.

With this we were able to determine the count of AF647-puncta and their total fluorescence intensity (Figure 12). Both read-outs show that spheroids at 24 hours post exposure to TZ-AF647 have approx. 3-fold more puncta and AF647 fluorescence intensity.

In this proof-of-concept experiment, we have shown that our imaging and analysis pipelines can be leveraged to quantify antibody internalization in cancer spheroids. This approach can be readily multiplexed with endolysosomal markers and perturbation experiments to dissect trafficking pathways and conduct efficacy studies.

Summary
In this case study we present a method to computationally quantify antibody internalization and trafficking to late endosomes from confocal microscopy images. We have applied this to real-time live imaging and to 3D cancer spheroids, demonstrating its general feasibility and the appropriateness of the ZEISS LSM 880 confocal microscope and ZEISS arivis Pro software for such experiments. If you want to reproduce the analysis or use this use case to learn more about arivis Pro, we have prepared some data sets and associated analysis pipeline for download below.

To finalize, we present some discussion points on how to further this experimental workflow.

A critical aspect of an antibody internalization assay is correctly identifying plasma membrane-bound vs. endosomal antibodies. Creating cells stably expressing endogenously-tagged GFP-Rab7a was key to obtain a reliable quantitative read-out of endocytosed and trafficked Trastuzumab. This could be furthered by multiplexing with markers that label the plasma membrane and additional endocytic compartments, thus enabling simpler plasma membrane-bound segmentation and increasing the scope of trafficking analysis. Furthermore, the different morphological appearance of plasma membrane-bound vs. endosomal antibody makes it a good candidate for a Deep Learning segmentation approach.

We also were able to quantify antibody internalization in cancer spheroids. This is noteworthy as 3D model systems like cancer spheroids can yield valuable data that directs in vivo translation, a major bottleneck in drug development. Moreover, many spheroids can be grown as co-cultures and therefore allow the study of processes involving cell-cell interactions. A drawback for imaging spheroids is the limited depth of imaging. Here, with the ZEISS LSM 880 confocal microscope, we were able to reach a depth of ~30 µm with sufficient resolution. If a greater imaging depth was required, we advise research to investigate using non-linear optics (also known as multiphoton), which is available with the ZEISS LSM 980 NLO confocal system.

Request the Trial Version of ZEISS arivis Pro

Download Case Study Files

[1] https://www.promega.de/resources/webinars/worldwide/archive/antibody-internalizationassay/

[2] https://www.creative-biolabs.com/drug-discovery/therapeutics/endocytosis-and-internalization-potency-detection.htm

[3] Vu T, Claret FX. Trastuzumab: updated mechanisms of action and resistance in breast cancer. Front Oncol. 2012 Jun 18;2:62. doi: 10.3389/fonc.2012.00062. PMID: 22720269; PMCID: PMC3376449

[4] Wang ZH, Zheng ZQ, Jia SC, Liu SN, Xiao XF, Chen GY, Liang WQ, Lu XF. Trastuzumab resistance in HER2-positive breast cancer: Mechanisms, emerging biomarkers and targeting agents. Front Oncol. 2022 Oct 6;12:1006429. doi: 10.3389/fonc.2022.1006429. PMID: 36276152; PMCID: PMC9584623

www.zeiss.com/microscopy